frontiers in Plant Science

ORIGINAL RESEARCH
published: 24 April 2020
doi: 10.3389/fpls.2020.00374

Quantifying Light Response of Leaf-Scale Water-Use Efficiency and Its Interrelationships With Photosynthesis and Stomatal Conductance in C_3 and C_4 Species

Zi-Piao Ye[1†], Yu Ling[2†], Qiang Yu[3,4,5], Hong-Lang Duan[6], Hua-Jing Kang[7], Guo-Min Huang[6], Shi-Hua Duan[8], Xian-Mao Chen[9], Yu-Guo Liu[10] and Shuang-Xi Zhou[11]**

[1] Maths & Physics College, Jinggangshan University, Ji'an, China, [2] College of Agricultural Sciences, Guangdong Ocean University, Zhanjiang, China, [3] State Key Laboratory of Soil Erosion and Dryland Farming on the Loess Plateau, Northwest A&F University, Yangling, China, [4] School of Life Sciences, University of Technology Sydney, Ultimo, NSW, Australia, [5] College of Resources and Environment, University of Chinese Academy of Science, Beijing, China, [6] Jiangxi Provincial Key Laboratory for Restoration of Degraded Ecosystems and Watershed Ecohydrology, Nanchang Institute of Technology, Nanchang, China, [7] Department of Landscape Architecture, Wenzhou Vocational College of Science & Technology, Wenzhou, China, [8] School of Life Sciences, Jinggangshan University, Ji'an, China, [9] Soil Fertilizer and Environmental Resources Institute, Jiangxi Academy of Agricultural Sciences, Nanchang, China, [10] Institute of Desertification Studies, Chinese Academy of Forestry, Beijing, China, [11] The New Zealand Institute for Plant and Food Research Limited, Havelock North, New Zealand

OPEN ACCESS

Edited by:
Fulai Liu,
University of Copenhagen, Denmark

Reviewed by:
Mathias Neumann Andersen,
Aarhus University, Denmark
Deliang Kong,
Henan Agricultural University, China

***Correspondence:**
Yu-Guo Liu
liuyuguo@caf.ac.cn
Shuang-Xi Zhou
shuangxi.zhou@plantandfood.co.nz

† These authors have contributed equally to this work

Specialty section:
This article was submitted to Plant Physiology, a section of the journal Frontiers in Plant Science

Received: *22 September 2019*
Accepted: *16 March 2020*
Published: *24 April 2020*

Citation:
Ye Z-P, Ling Y, Yu Q, Duan H-L, Kang H-J, Huang G-M, Duan S-H, Chen X-M, Liu Y-G and Zhou S-X (2020) Quantifying Light Response of Leaf-Scale Water-Use Efficiency and Its Interrelationships With Photosynthesis and Stomatal Conductance in C_3 and C_4 Species. Front. Plant Sci. 11:374. doi: 10.3389/fpls.2020.00374

Light intensity (I) is the most dynamic and significant environmental variable affecting photosynthesis (A_n), stomatal conductance (g_s), transpiration (T_r), and water-use efficiency (WUE). Currently, studies characterizing leaf-scale WUE–I responses are rare and key questions have not been answered. In particular, (1) What shape does the response function take? (2) Are there maximum intrinsic (WUE_i; WUE_{i-max}) and instantaneous WUE (WUE_{inst}; $WUE_{inst-max}$) at the corresponding saturation irradiances (I_{i-sat} and $I_{inst-sat}$)? This study developed WUE_i–I and WUE_{inst}–I models sharing the same non-asymptotic function with previously published A_n–I and g_s–I models. Observation-modeling intercomparison was conducted for field-grown plants of soybean (C_3) and grain amaranth (C_4) to assess the robustness of our models versus the non-rectangular hyperbola models (NH models). Both types of models can reproduce WUE–I curves well over light-limited range. However, at light-saturated range, NH models overestimated WUE_{i-max} and $WUE_{inst-max}$ and cannot return I_{i-sat} and $I_{inst-sat}$ due to its asymptotic function. Moreover, NH models cannot describe the down-regulation of WUE induced by high light, on which our models described well. The results showed that WUE_i and WUE_{inst} increased rapidly within low range of I, driven by uncoupled photosynthesis and stomatal responsiveness. Initial response rapidity of WUE_i was higher than WUE_{inst} because the greatest increase of A_n and T_r occurred at low g_s. C_4 species showed higher WUE_{i-max} and $WUE_{inst-max}$ than C_3 species—at similar I_{i-sat} and $I_{inst-sat}$. Our intercomparison highlighted larger discrepancy between WUE_i–I and WUE_{inst}–I responses in C_3 than C_4 species, quantitatively characterizing an

important advantage of C_4 photosynthetic pathway—higher A_n gain but lower T_r cost per unit of g_s change. Our models can accurately return the wealth of key quantities defining species-specific WUE–*I* responses—besides A_n–*I* and g_s–*I* responses. The key advantage is its robustness in characterizing these entangled responses over a wide *I* range from light-limited to light-inhibitory light intensities, through adopting the same analytical framework and the explicit and consistent definitions on these responses. Our models are of significance for physiologists and modelers—and also for breeders screening for genotypes concurrently achieving maximized photosynthesis and optimized WUE.

Keywords: irradiance, leaf gas exchange, light response curve, maximum water use efficiency, model, plant functional type (PFT), saturation light intensity, transpiration

INTRODUCTION

Stomata control the balance between carbon flux driven by photosynthesis and water flux dominated by transpiration, which is characterized by water-use efficiency (WUE) at various scales (Sinclair et al., 1984; Gilbert et al., 2011; Eamus et al., 2016; Medlyn et al., 2017). WUE can thus indicate the natural selection on the balance between these fluxes (Hetherington and Woodward, 2003). Characterizing the environmental impacts on WUE among plant species and/or plant function types can advance our knowledge on differential plant adaptation strategies, and improve our prediction on consequences of environmental challenges (Avola et al., 2008; Egea et al., 2011; Zhou et al., 2014, 2016; De Kauwe et al., 2015; Köhler et al., 2016; Ahrar et al., 2017). For instance, plant species with the highest WUE would show the greatest fitness in dry habitats (Dudley, 1996; Zhou et al., 2019). WUE is also an important metric in crop breeding and genotype selection, especially for irrigated crops whose water use significantly affects crop productivity and profitability (Duursma et al., 2013; Flexas et al., 2013; Bota et al., 2016; Webster et al., 2016).

WUE can be estimated using different techniques, based on observations of leaf gas exchange, stable isotope discrimination, and eddy covariance fluxes (Medlyn et al., 2017). Among these techniques, WUE is most commonly estimated by measuring leaf gas exchange, facilitated by portable photosynthesis system allowing simultaneous measurement of leaf-scale carbon and water fluxes (Medrano et al., 2015). WUE derived from leaf gas exchange measurement is usually defined as the ratio of net CO_2 assimilation rate (A_n) to stomatal conductance for water vapor (g_s)—intrinsic water-use efficiency (WUE_i; von Caemmerer and Farquhar, 1981), or the ratio of A_n to transpiration rate (T_r)—instantaneous water-use efficiency (WUE_{inst}; Fischer and Turner, 1978) (see **Table 1** for a summary of parameters and units). WUE_i can be used to compare photosynthetic characteristics independently of evaporative demand (Linares and Camarero, 2012). WUE_{inst} is a key determinant of whole-plant WUE as it summarizes plant dry mass production per unit of water loss (Sinclair et al., 1984; Duursma et al., 2013; but see Medrano et al., 2015 for constraints). WUE_i and WUE_{inst} have been widely used as an index of plant and vegetation performances in response to various environmental changes, such as changed water or light availabilities, vapor pressure deficit (VPD), temperature and CO_2 concentration (Aranda et al., 2007; Avola et al., 2008; Linares and Camarero, 2012; Duursma et al., 2013; Bota et al., 2016).

Light is often viewed as the most significant environmental variable affecting photosynthesis, stomatal behavior and WUE (Knapp and Smith, 1987; Aranda et al., 2007; McAusland et al., 2016). Plants in most ecosystems experience rapid short-term variability in light resource (Smith et al., 1989), which can cause continual transition of A_n, g_s, T_r, WUE_i, and WUE_{inst} throughout the growing season (Knapp and Smith, 1990; Knapp, 1993). However, studies characterizing the light response of WUE are rare (McAusland et al., 2016). It is largely unknown whether there is a maximum WUE_i or WUE_{inst}—and the corresponding saturation irradiance—for plants under dynamic irradiance conditions, or how plant species or plant function types (PFTs) would differ in their light responses of WUE_i and WUE_{inst}.

Characterization of the interrelationships among light responses of A_n, g_s, T_r, WUE_i and WUE_{inst}—which can be simultaneously measured—will be fundamental to the scaling-up modeling of WUE–*I* responses at the whole-plant and ecosystem scale. The foremost step toward this direction calls for a robust model, with which (1) the WUE_i and WUE_{inst} responses to a gradient of irradiance intensity (*I*) levels (WUE_i–*I* and WUE_{inst}–*I* response curve, respectively) can be characterized, and (2) the key quantities defining the response curves—such as the initial slope of the response curve, the maximum WUE and the corresponding saturation irradiance—can be quantified. Ideally, the model can accurately represent the differential WUE_i and WUE_{inst} responses among plant species or PFTs, such as that reported between C_3 and C_4 species with contrasting light responses of photosynthesis, stomatal functioning, and WUE (Pearcy and Ehleringer, 1984; Knapp, 1993). For a given A_n, g_s and T_r are higher in C_3 than C_4 plants, leading to higher WUE_i and WUE_{inst} in C_4 plants, which has higher utilization efficiency of CO_2 at relatively lower intercellular CO_2 concentration (Pearcy and Ehleringer, 1984). The objectives of this study were to develop a leaf-scale WUE–*I* model and assess the model performance against experimental field observations of C_3 and C_4 species in order to answer key questions of how best to model the light response of WUE_i and WUE_{inst}. In particular: (1) What shape does the leaf-scale WUE–*I* response function

TABLE 1 | List of major model parameters defining the light response curves of photosynthesis (A_n), stomatal conductance (g_s), intrinsic water use efficiency (WUE_i), and instantaneous water use efficiency (WUE_{inst}).

Symbol	Definition	Unit
A_n	Net photosynthetic rate	μmol CO_2 m^{-2} s^{-1}
A_{nmax}	Maximum net photosynthetic rate	μmol CO_2 m^{-2} s^{-1}
g_s	Stomatal conductance	mol H_2O m^{-2} s^{-1}
g_{s-max}	Maximum stomatal conductance	mol H_2O m^{-2} s^{-1}
I	Light intensity	μmol photons m^{-2} s^{-1}
I_{sat}	Saturation light intensity corresponding to maximum net photosynthetic rate	μmol photons m^{-2} s^{-1}
I_{g-sat}	Saturation light intensity corresponding to maximum stomatal conductance	μmol photons m^{-2} s^{-1}
I_{i-sat}	Saturation light intensity corresponding to maximum intrinsic water-use efficiency	μmol photons m^{-2} s^{-1}
$I_{inst-sat}$	Saturation light intensity corresponding to maximum instantaneous water-use efficiency	μmol photons m^{-2} s^{-1}
R_d	Mitochondrial CO_2 release in the dark	μmol CO_2 m^{-2} s^{-1}
T_r	Transpiration rate	mmol H_2O m^{-2} s^{-1}
WUE_i	Intrinsic water-use efficiency	μmol CO_2 mol^{-1} H_2O
WUE_{i-max}	Maximum intrinsic water-use efficiency	μmol CO_2 mol^{-1} H_2O
WUE_{inst}	Instantaneous water-use efficiency	μmol CO_2 $mmol^{-1}$ H_2O
$WUE_{inst-max}$	Maximum instantaneous water-use efficiency	μmol CO_2 $mmol^{-1}$ H_2O
α, α_0, α_1, α_2	Initial slope of light response curve of A_n, g_s, WUE_i and WUE_{inst}	mmol H_2O m^{-2} s^{-1}
β, β_0, β_1, β_2	Inhibitor coefficient of light response curve of A_n, g_s, WUE_i and WUE_{inst}	m^2 s μmol^{-1} photons
γ, γ_0, γ_1, γ_2	Saturation coefficient of light response curve of A_n, g_s, WUE_i and WUE_{inst}	m^2 s μmol^{-1} photons
K_i	Residual intrinsic water-use efficiency	μmol CO_2 mol^{-1} H_2O
K_{inst}	Residual instantaneous water-use efficiency	μmol CO_2 $mmol^{-1}$ H_2O

take? Is there a maximum WUE_i and/or WUE_{inst}—and the corresponding saturation irradiances for plants under dynamic irradiance conditions? (2) Can the model well represent the differential WUE_i–I and/or WUE_{inst}–I response characteristics between C_3 and C_4 species? By integrating the published A_n–I (Ye, 2007; Ye et al., 2013) and g_s–I (Ye and Yu, 2008) response function, we developed an explicit WUE–I modeling framework and hypothesized that the species-specific light response curves of WUE_i and WUE_{inst} can be quantitatively characterized using the same non-asymptotic function. The hypothesis was tested using an observation-modeling intercomparison on WUE_i–I and WUE_{inst}–I responses for field-grown C_3 [soybean (*Glycine max* L.)] and C_4 species [grain amaranth (*Amaranthus hypochondriacus* L.)] under high I condition in the growing season. Model performance against that of the non-rectangular hyperbola model was also evaluated.

MATERIALS AND METHODS

Analytical Models

A non-asymptotic model has been previously developed and tested to well characterize the light response of photosynthesis (Ye, 2007; Ye et al., 2013), with its simplified form as follows:

$$A_n = \alpha \frac{1-\beta I}{1+\gamma I} I\text{-}R_d \quad (1)$$

where α is the initial slope of light response curve of photosynthesis, I is the irradiance, and β and γ are the photoinhibition coefficient and saturation coefficient, respectively, and R_d is the dark respiratory rate. The key model parameters are listed in **Table 1**.

The saturation irradiance (I_{sat}) corresponding to the light-saturated photosynthetic rate (A_{nmax}) can be calculated as follows:

$$I_{sat} = \frac{\sqrt{(\beta+\gamma)/\beta} - 1}{\gamma} \quad (2)$$

$$A_{nmax} = \alpha \left(\frac{\sqrt{\beta+\gamma} - \sqrt{\beta}}{\gamma} \right)^2 - R_d \quad (3)$$

Eq. 1 has been widely used to characterize photosynthetic light response curves of various plant species under different environmental conditions, highlighting its better performance than that of rectangular (Baly, 1935) and non-rectangular hyperbolic models (Thornley, 1976; Wargent et al., 2011; Xu et al., 2012a,b; Song et al., 2015; Chen et al., 2016). The rectangular and the non-rectangular hyperbolic models have been reported to overestimate A_{nmax} (dos Santos et al., 2013), and cannot quantify I_{sat} (Gomes et al., 2006; dos Santos et al., 2013; Song et al., 2015; Chen et al., 2016).

Meanwhile, a model of the same non-asymptotic form as Eq. 1 has been developed and tested to well characterize the light response of stomatal conductance (Ye and Yu, 2008), as follows:

$$g_s = \alpha_0 \frac{1-\beta_0 I}{1+\gamma_0 I} I + g_{s0} \quad (4)$$

where α_0 is the initial slope of light response curve of stomatal conductance, g_{s0} is the residual stomatal conductance, and β_0 and γ_0 are two coefficients that are independent of I (Ye and Yu, 2008). Most existing stomatal conductance models cannot quantify the g_{s-max} or the corresponding I_{g-sat} under changing irradiance conditions (Dewar, 2002; Buckley et al., 2003; Buckley and Mott, 2013; Flexas et al., 2013).

The g_s–I model developed by Ye and Yu (2008) can well characterize the g_s–I response, from which key parameters defining the g_s–I response—such as g_{s-max} and I_{g-sat}—can be easily obtained.

The saturation irradiance (I_{g-sat}) corresponding to the light-saturated stomatal conductance (g_{s-max}) can be calculated as follows:

$$I_{g-sat} = \frac{\sqrt{(\beta_0 + \gamma_0)/\beta_0} - 1}{\gamma_0} \quad (5)$$

$$g_{smax} = \alpha_0 \left(\frac{\sqrt{\beta_0 + \gamma_0} - \sqrt{\beta_0}}{\gamma_0} \right)^2 + g_{s0} \quad (6)$$

Here, we hypothesize that the light response of WUE_i can be characterized using the same non-asymptotic form as that of the A_n–I (Eq. 1) and g_s–I (Eq. 4) response functions, as follows:

$$WUE_i = \alpha_1 \frac{1 - \beta_1 I}{1 + \gamma_1 I} I - K_i \quad (7)$$

where α_1 represents the initial slope of light response curve of WUE_i, β_1, and γ_1 are coefficients that are independent of I, and K_i is the residual intrinsic water-use efficiency. The saturation irradiance (I_{i-sat}) corresponding to the maximum WUE_i (WUE_{i-max}) can be calculated as follows:

$$I_{i-sat} = \frac{\sqrt{(\beta_1 + \gamma_1)/\beta_1} - 1}{\gamma_1} \quad (8)$$

$$WUE_{i-max} = \alpha_1 \left(\frac{\sqrt{\beta_1 + \gamma_1} - \sqrt{\beta_1}}{\gamma_1} \right)^2 - K_i \quad (9)$$

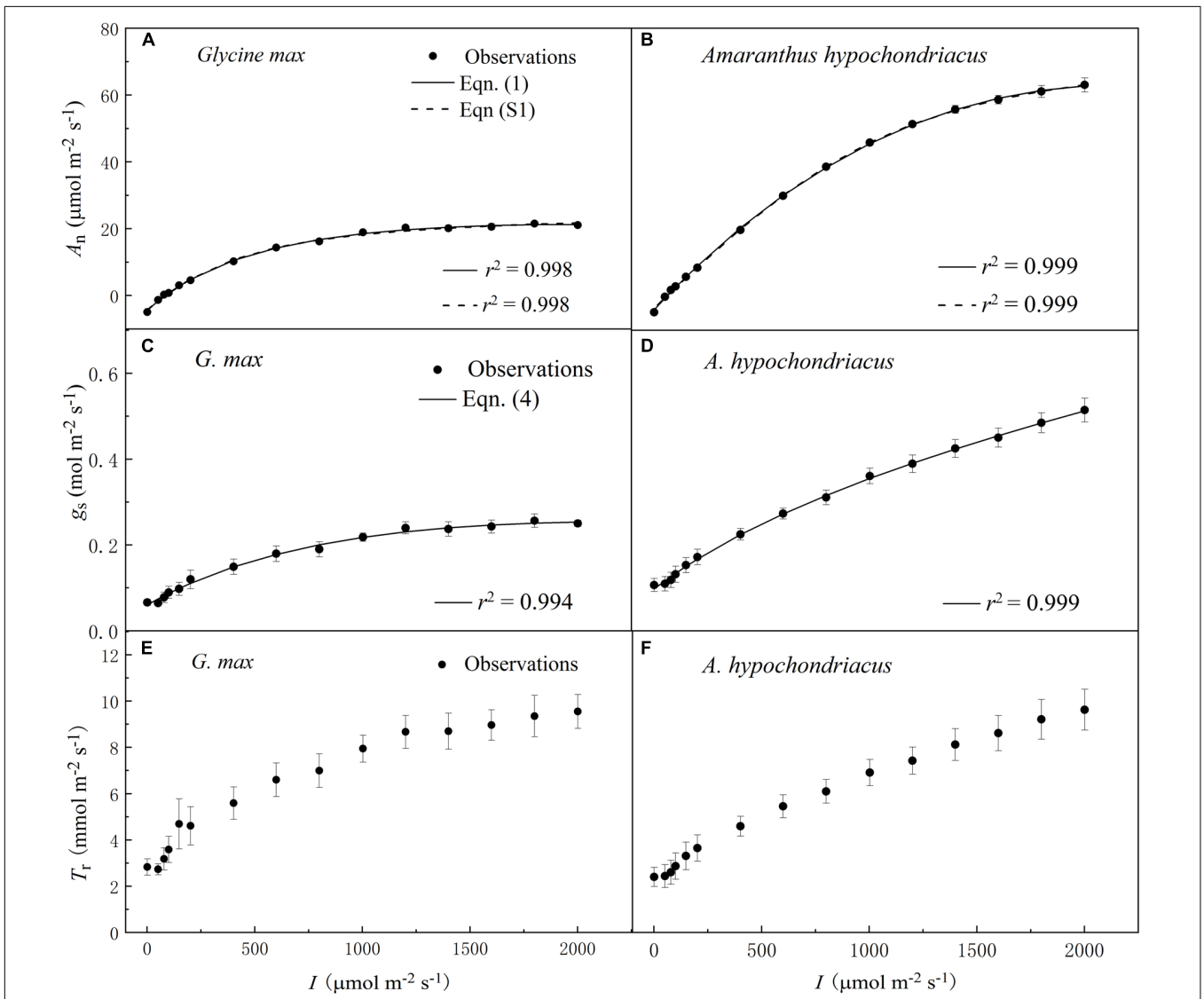

FIGURE 1 | Irradiance (I) responses of net photosynthetic rate (A_n) **(A,B)**, stomatal conductance (g_s) **(C,D)** and transpiration rate (T_r) **(E,F)** for C_3 [soybean (*Glycine max*)] and C_4 species [grain amaranth (*Amaranthus hypochondriacus*)], respectively. In plots **(A)** and **(B)**, solid lines were fitted using Eq. 1 and dashed lines were fitted using the non-rectangular hyperbola model (Eq. S1). In plots **(C)** and **(D)**, solid lines were fitted using Eq. 4. Data are the mean ± SE (n = 4).

TABLE 2 | Fitted (Eq. 1) and measured (Obs.) values of parameters defining the light response curve of photosynthesis for C_3 (soybean) and C_4 species (grain amaranth).

Species	α		A_{nmax} (μmol m^{-2} s^{-1})		I_{sat} (μmol m^{-2} s^{-1})		β (m^2 s μmol^{-1})		γ (m^2 s μmol^{-1})		R_d (μmol m^{-2} s^{-1})	
	Eq. 1	Obs.	Eq. 1	Obs.	Eq. 1	Obs.	Eq. 1	Obs.	Eq. 1	Obs.	Eq. 1	Obs.
Soybean	0.059 ± 0.005^a	–	21.25 ± 0.53^b	21.79 ± 0.58	1925.38 ± 60.30^a	1800.00 ± 81.65	$(1.20 \pm 0.10) \times 10^{-4}$	–	$(1.25 \pm 0.16) \times 10^{-3}$	–	4.36 ± 0.46^a	4.90 ± 0.29^a
Grain amaranth	0.069 ± 0.001^a	–	63.36 ± 2.46^a	–	2186.67 ± 101.21^a	–	$(2.07 \pm 0.15) \times 10^{-4}$	–	$(1.08 \pm 0.29) \times 10^{-4}$	–	4.18 ± 0.35^a	4.99 ± 0.30^a

The parameters are initial slope of the A_n–I curve (α), the maximum net photosynthetic rate (A_{nmax}) and the corresponding saturation irradiance (I_{sat}), photoinhibition coefficient (β), saturation coefficient (γ), and dark respiration rate (R_d). All values are the means ± SE (n = 4). Different letters denote statistically significant differences ($P \leq 0.05$) between soybean and grain amaranth within each column of fitted (Eq. 1) or measured (Obs.) values. There is no statistically significant difference between fitted (Eq. 1) and measured (Obs.) values for each parameter. See ***Table 1*** *for definitions of abbreviations.*

Since g_s controls leaf T_r at a given *VPD* (Duursma et al., 2013), we hypothesize that the light response of WUE_{inst} can also be characterized using the same non-asymptotic function as that of WUE_i–I response function (Eq. 7), as follows:

$$WUE_{inst} = \alpha_2 \frac{1 - \beta_2 I}{1 + \gamma_2 I} I - K_{inst} \tag{10}$$

where α_2 represents the initial slope of light response curve of WUE_{inst}, β_2 and γ_2 are coefficients that are independent of I, and K_{inst} is the residual instantaneous water-use efficiency. The saturation irradiance ($I_{inst-sat}$) corresponding to the maximum WUE_{inst} ($WUE_{inst-max}$) can be calculated as follows:

$$I_{inst-sat} = \frac{\sqrt{(\beta_2 + \gamma_2)/\beta_2} - 1}{\gamma_2} \tag{11}$$

$$WUE_{inst-max} = \alpha_2 \left(\frac{\sqrt{\beta_2 + \gamma_2} - \sqrt{\beta_2}}{\gamma_2} \right)^2 - K_{inst} \tag{12}$$

In this study, we tested if Eqs. 7 and 10 can well characterize the species-specific WUE–I response characteristics against model-oriented field observations and the simulations using the non-rectangular hyperbola model—in terms of the initial slope of light response curve of WUE (α_1 and α_2, respectively), the maximum WUE_{inst} (WUE_i and $WUE_{inst-max}$, respectively), and the saturation irradiance (I_{i-sat} and $I_{inst-sat}$, respectively).

Study Site and Plant Material

The field observations on one C_3 species—soybean (*Glycine max* L.) and one C_4 species—grain amaranth (*A. hypochondriacus* L.) were conducted at the Yucheng Comprehensive Experiment Station of the Chinese Academy of Sciences, located at the irrigation district of the Yellow River Basin in the North China Plain. This region is dominated by the warm-temperate semi-humid monsoon climate and is suitable for planting soybean and grain amaranth with high yields. This region has ample energy resource, and the light intensity in the growing season usually reaches ∼2000 μmol m^{-2} s^{-1} in sunny days. Soybean and grain amaranth were planted in field on May 3rd and June 15th 2012, respectively. All plants were kept under moist condition throughout the experiment.

Light Response Curve Measurement

The leaf gas exchange measurements were conducted after 45 days of growth in field—June 16th for soybean and July 29th for grain amaranth. Fully expanded sun-exposed leaves of four plants for each species were measured using a portable photosynthesis system (LI-6400, Li-Cor Inc., Lincoln, NE, United States). Before each measurement, the leaf was acclimated in the chamber to achieve stable gas exchange, with reference CO_2 concentration maintained at 380 μmol CO_2 mol^{-1}, irradiance intensity maintained at 2000 μmol photon m^{-2} s^{-1}, and leaf temperature maintained at 35°C. After the leaf acclimated to the cuvette environment, the photosynthetic light response curve measurements were conducted with a descending gradient of irradiance intensity

TABLE 3 | Fitted (Eq. 4) and measured (Obs.) values of parameters defining the light response curve of stomatal conductance for C_3 (soybean) and C_4 species (grain amaranth).

Species	α_0		g_{s-max} (mol m^{-2} s^{-1})		I_{g-sat} (μmol m^{-2} s^{-1})		β_0 (m^2 s μmol^{-1})		γ_0 (m^2 s μmol^{-1})		g_{s0} (mol m^{-2} s^{-1})	
	Eq. 4	Obs.	Eq. 4	Obs.	Eq. 4	Obs.	Eq. 4	Obs.	Eq. 4	Obs.	Eq. 4	Obs.
Soybean	$(3.5 \pm 0.9) \times 10^{-4a}$	–	0.26 ± 0.01	0.26 ± 0.02	2291.90 ± 259.17	1800.00 ± 81.65	$(1.7 \pm 0.7) \times 10^{-4}$	–	$(8.6 \pm 5.5) \times 10^{-4}$	–	0.06 ± 0.01^a	0.07 ± 0.01^a
Grain amaranth	$(7.3 \pm 3.0) \times 10^{-4a}$	–	–	–	–	–	$(-5.6 \pm 6.1) \times 10^{-4}$	–	$(6.1 \pm 5.5) \times 10^{-3}$	–	0.09 ± 0.01^a	0.11 ± 0.02^a

The parameters are initial slope of the g_s–I curve (α_0), coefficients β_0 and γ_0, the maximum stomatal conductance (g_{s-max}) and the corresponding saturation irradiance (I_{g-sat}), and the residual stomatal conductance (g_{s0}). All values are the means ± SE ($n = 4$). Different letters denote statistically significant differences ($P \leq 0.05$) between soybean and grain amaranth within each column of fitted (Eq. 4) or measured (Obs.) values. There is no statistically significant difference between fitted (Eq. 4) and measured (Obs.) values for each parameter. See ***Table 1*** *for definitions of abbreviations.*

levels, as follows: 2000, 1800, 1600, 1400, 1200, 1000, 800, 600, 400, 200, 150, 100, 80, 50, and 0 μmol m^{-2} s^{-1}. At each irradiance level, leaf gas exchange was monitored to ensure reaching steady-state plateau before data-logging. *VPD* was kept stable during measurements (**Supplementary Figure S1**). The A_n–I, g_s–I, WUE_i–I, and WUE_{inst}–I response curves were fitted by Eqs. 1, 4, 7, and 10, respectively. I_{sat}, I_{g-sat}, I_{i-sat}, and $I_{inst-sat}$ values were calculated following Eqs. 2, 5, 8, and 11, respectively. A_{nmax}, g_{s-max}, WUE_{i-max}, and $WUE_{inst-max}$ values were calculated following Eqs. 3, 6, 9, and 12, respectively.

Data Analysis

All statistical tests were performed using the statistical package SPSS 18.5 statistical software (SPSS, Chicago, IL, United States). The analysis of variance (ANOVA) was used to assess species effects. Paired-sample *t* tests were conducted to test whether there were significant differences between fitted and measured values of quantitative traits (α, A_{nmax}, I_{sat}, α_0, g_{s-max}, I_{g-sat}, α_1, WUE_{i-max}, I_{i-sat}, α_2, $WUE_{inst-max}$, $I_{inst-sat}$, etc.). Goodness of fit of the mathematical model to experimental observations was assessed using the coefficient of determination ($r^2 = 1 - SSE/SST$, where *SST* is the total sum of squares and *SSE* is the error sum of squares).

RESULTS

Light Response Curves of A_n, g_s, and T_r

The increase of I led to a rapid initial increase of A_n (**Figures 1A,B**), g_s (**Figures 1C,D**), and T_r (**Figures 1E,F**) for both C_3 and C_4 species. However, the initial increase rate of A_n was 100-fold higher than that of g_s for both species (**Tables 2** and **3**). The high coefficient of determination (r^2) values indicated that the species-specific A_n–I response curves fitted by Eq. 1—and the g_s–I response curves fitted by Eq. 4—were highly representative of the observations for both species (**Figure 1**).

Soybean exhibited a single-peaked pattern for both A_n–I and g_s–I responses, characterized by the increase of A_n and g_s with the increasing I until reaching the A_{nmax} and g_{s-max} at the corresponding I_{sat} and I_{g-sat}, respectively (**Figures 1A,C** and **Tables 2** and **3**). Compared with Eq. 1, the non-rectangular hyperbola model (**Supplementary Eq. S1**) showed similarly high r^2 value in simulating A_n–I response curves but significantly overestimated the A_{nmax} (**Figures 1A,B** and **Supplementary Table S1**). Paired-sample *t* tests showed there were no significant differences between the fitted values and the measured values of A_{nmax}, I_{sat}, g_{s-max}, and I_{g-sat} for soybean (**Tables 2** and **3**). Grain amaranth kept increasing its A_n and g_s within the range of irradiance intensity applied during measurements (0–2000 μmol photon m^{-2} s^{-1}), without showing an observational A_{nmax}, I_{sat}, g_{s-max}, or I_{g-sat} (**Figures 1B,D** and **Tables 2** and **3**). Grain amaranth showed relatively higher (not significant) initial increase rate of g_s, characterized by an initial slope of the light response curve of g_s (α_0) (**Figure 1** and **Tables 2** and **3**).

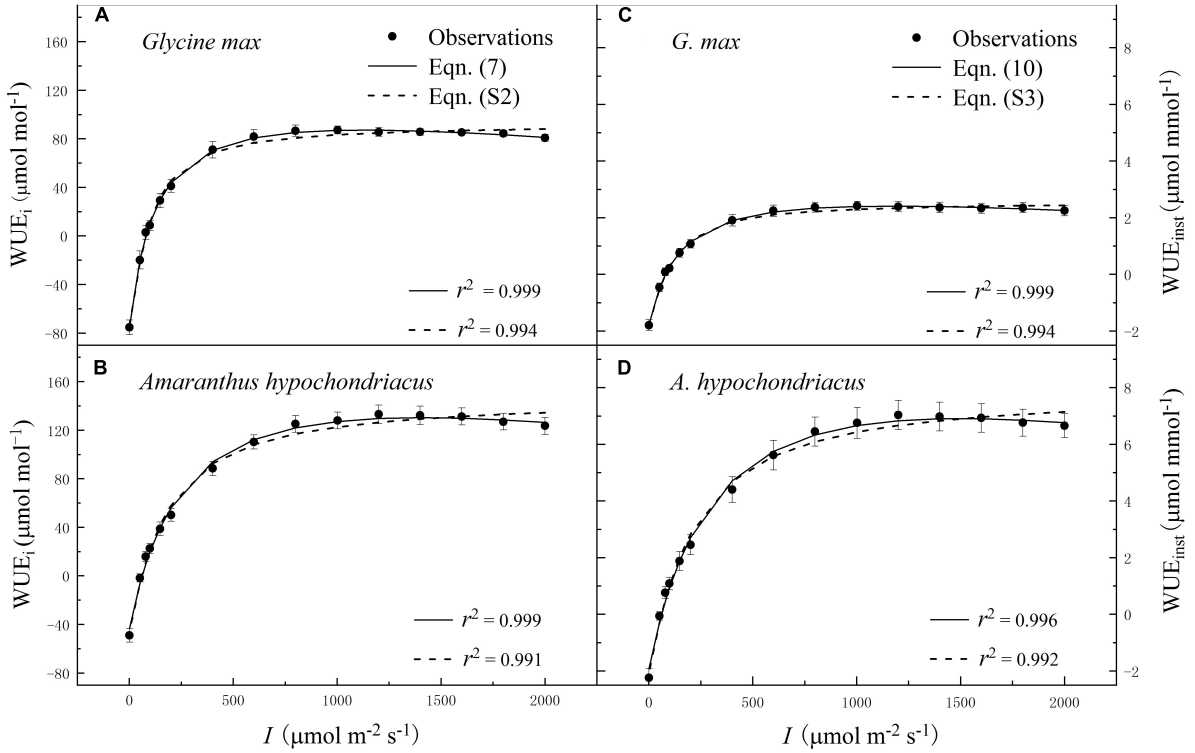

FIGURE 2 | Irradiance (*I*) response of intrinsic water-use efficiency (WUE_i) **(A,B)** and instantaneous water-use efficiency (WUE_{inst}) **(C,D)** for C_3 [soybean (*Glycine max*)] and C_4 species [grain amaranth (*Amaranthus hypochondriacus*)], respectively. In plots **(A)** and **(B)**, solid lines were fitted using Eq. 7 and dashed lines were fitted using the non-rectangular hyperbola model (Eq. S2). In plots **(C)** and **(D)**, solid lines were fitted using Eq. 10 and dashed lines were fitted using the non-rectangular hyperbola model (Eq. S3). Data are the mean ± SE (n = 4).

Light Response Curves of WUE_i and WUE_{inst}

Within the low range of irradiance intensity, WUE_i and WUE_{inst} of both species increased almost linearly with the increasing *I*. Both soybean and grain amaranth exhibited a single-peaked WUE_i–*I* and WUE_{inst}–*I* response pattern, respectively. In particular, both species showed an increase of WUE_i and WUE_{inst} with the increasing *I* until reaching the species-specific WUE_{i-max} and $WUE_{inst-max}$ at the corresponding species-specific saturation irradiance levels (I_{i-sat} and $I_{inst-sat}$, respectively) (**Figure 2** and **Tables 4** and **5**). However, soybean showed significantly lower observed and fitted WUE_{i-max} and $WUE_{inst-max}$ ($P \leq 0.05$) than grain amaranth (**Figure 2** and **Tables 4** and **5**). The two species showed no significant difference in I_{i-sat}, $I_{inst-sat}$ or the initial increase rate of WUE_i or WUE_{inst}—characterized by a maximal slope of the light response curves (α_1 and α_2, respectively) (**Figure 2** and **Tables 4** and **5**).

The high r^2 values indicated that WUE_i–*I* response curves fitted by Eq. 7—and the WUE_{inst}–*I* response curves fitted by Eq. 10—were highly representative of the observations of both species (**Figure 2** and **Tables 4** and **5**). There were no significant differences between fitted and observed values in WUE_{i-max}, $WUE_{inst-max}$, I_{i-sat}, $I_{inst-sat}$, K_i, or K_{inst} (**Tables 4** and **5**). Compared with Eqs. 7 and 10, the non-rectangular hyperbola model (**Supplementary Eqs. S2 and S3**, respectively) showed similarly high r^2 values but significantly overestimated WUE_{i-max} and $WUE_{inst-max}$ for the two species (**Supplementary Tables S2 and S3**).

Discussion

Our WUE_i–*I* and WUE_{inst}–*I* models represented cultivar-specific response curves over a wide range of light intensities extremely well ($r^2 \geq 0.996$), including the decline of WUE_i and WUE_{inst} beyond the saturation irradiances which the NH models cannot represent due to the asymptotic function. Our models can also return values for WUE_{i-max}, $WUE_{inst-max}$, I_{i-sat}, and $I_{inst-sat}$, which were in very close agreement with the measured values. The NH models cannot characterize the decline in WUE_i and WUE_{inst} induced by high light, leading to overestimations of WUE_{i-max} and $WUE_{inst-max}$ (**Supplementary Tables S2 and S3**).

Interrelationships of Light Responses of Photosynthesis, Stomatal Conductance, and Water-Use Efficiency

WUE_i and WUE_{inst} increased rapidly within low range of *I*, mainly driven by the uncoupled rapidity of photosynthetic and stomatal responses (**Figures 1**, **2** and **Tables 4** and **5**; Knapp and Smith, 1990; McAusland et al., 2016). In this study, both C_3 and

TABLE 4 | Fitted (Eq. 7) and measured (Obs.) values of parameters defining the light response curve of intrinsic water-use efficiency for C_3 (soybean) and C_4 species (grain amaranth).

Species	α_1		WUE_{i-max} (μmol mol^{-1})		I_{i-sat} (μmol m^{-2} s^{-1})		β_1 (m^2 s μmol^{-1})		γ_1 (m^2 s μmol^{-1})		K_i (μmol mol^{-1})	
	Eq. 7	Obs.	Eq. 7	Obs.	Eq. 7	Obs.	Eq. 7	Obs.	Eq. 7	Obs.	Eq. 7	Obs.
Soybean	1.53 ± 0.25^a	–	87.66 ± 3.38^b	89.24 ± 3.26^b	1153.95 ± 101.89^a	1250.00 ± 262.99^a	(8.49 ± 0.62) × 10^{-5}	–	(7.52 ± 0.89) × 10^{-3}	–	74.92 ± 6.16^a	75.35 ± 5.98^a
Grain amaranth	0.87 ± 0.19^a	–	131.32 ± 7.83^a	133.99 ± 7.63^a	1417.60 ± 90.68^a	1150.00 ± 125.83^a	(1.21 ± 0.30) × 10^{-4}	–	(3.72 ± 1.26) × 10^{-3}	–	40.35 ± 4.24^b	49.03 ± 5.69^b

The parameters are initial slope of the WUE_i–I curve (α_1), the maximum intrinsic water-use efficiency (WUE_{i_max}) and the corresponding saturation irradiance (I_{i_sat}), and coefficients β_1 and γ_1 and K_i. All values are the means ± SE (n = 4). Different letters denote statistically significant differences ($P \leq 0.05$) between soybean and grain amaranth within each column of fitted (Eq. 7) or measured (Obs.) values. There is no statistically significant difference between fitted (Eq. 7) and measured (Obs.) values for each parameter. See ***Table 1*** *for definitions of abbreviations.*

C_4 species showed 100-fold higher initial increase rate of A_n (α) than that of g_s (α_0) (**Tables 2** and **3**). The rapid initial increase of WUE_i and WUE_{inst}—characterized by α_1 and α_2, respectively—occurred at low g_s (and at low I), when small increase in g_s exerted the greatest impacts on A_n and T_r (Hetherington and Woodward, 2003). The occurrence of the greatest A_n and T_r increase at low g_s also determined that α_1 would be much higher than α_2 for a given species (**Figure 2** and **Tables 4** and **5**).

With the increasing I (from 0 to ∼800 μmol m^{-2} s^{-1}), faster photosynthesis response than stomatal response led to the decline of intercellular CO_2 concentration (C_i) (**Supplementary Figure S1**; McAusland et al., 2016), causing further opening of stomatal pores (Mott, 1988) which allowed for diffusion of ambient CO_2 into the leaf (Hetherington and Woodward, 2003). Further increase of g_s—beyond the low g_s range—led to minimal increase of A_n and T_r (Hetherington and Woodward, 2003), such that WUE_i and WUE_{inst} flattened quickly after reaching the WUE_{i-max} and $WUE_{inst-max}$ (**Figure 2**). Further increase of I beyond I_{i-sat} and $I_{inst-sat}$ led to a decrease in WUE_i and WUE_{inst}. To reach A_{nmax}, both soybean and grain amaranth would have to show a decrease of WUE_i (or WUE_{inst}) from WUE_{i-max} (or $WUE_{inst-max}$) (**Figures 1**, **2**).

Differential Light Responses of Water-Use Efficiency Between C_3 and C_4 Species

The observation-modeling intercomparison in this study highlighted the differential single-peaked WUE_i–I and WUE_{inst}–I responses—besides differential A_n–I and g_s–I responses—between C_3 and C_4 species (**Figure 2** and **Tables 4** and **5**). C_4 species (grain amaranth) showed higher WUE_i and WUE_{inst} than C_3 species (soybean), suggesting its better leaf-scale optimization of carbon uptake versus water loss than C_3 species (**Figures 1**, **2** and **Tables 2**, **4**, and **5**). This may be due to higher photosynthetic capacity and rapidity of stomatal response (α_0) in C_4 species under changing irradiance conditions (**Figure 1** and **Tables 2** and **3**), which facilitate relatively closer coupling between A_n and g_s in C_4 species than C_3 species (McAusland et al., 2016).

Moreover, this study identifies greater interspecific difference in WUE_{inst} than that in WUE_i—at high I range when WUE_i and WUE_{inst} flatten (**Figure 2** and **Tables 4** and **5**). C_3 species (soybean) showed larger discrepancy between its WUE_i–I and WUE_{inst}–I responses than that of C_4 species (grain amaranth). This may be due to differential water use strategies between C_3 and C_4 species—C_4 species holds smaller T_r change per unit of g_s change in relative to C_3 species (Knapp, 1993). These results quantitatively demonstrate that the differential WUE_i–I responses between C_3 and C_4 species would not necessarily mirror their differential WUE_{inst}–I responses (**Figure 2**).

These results support previous studies reporting that water conservation—in terms of high WUE—is an important consequence of the C_4 photosynthetic pathway (besides high carbon gain rate) at different scales including single leaf, whole plant, and even whole communities (Ludlow and Wilson, 1972),

TABLE 5 | Fitted (Eq. 10) and measured (Obs.) values of parameters defining the light response curve of instantaneous water-use efficiency for C_3 (soybean) and C_4 species (grain amaranth).

Species	α_2		$WUE_{inst-max}$ (μmol mmol^{-1})		$I_{inst-sat}$ (μmol m^{-2} s^{-1})		β_2 (m^2 s μmol^{-1})		γ_2 (m^2 s μmol^{-1})		K_{inst} (μmol mmol^{-1})	
	Eq. 10	Obs.	Eq. 10	Obs.	Eq. 10	Obs.	Eq. 10	Obs.	Eq. 10	Obs.	Eq. 10	Obs.
Soybean	0.035 ± 0.006^a	–	2.42 ± 0.17^b	2.47 ± 0.16^b	1182.74 ± 63.01^a	1300.00 ± 191.49^a	$(9.38 \pm 1.29) \times 10^{-5}$	–	$(6.34 \pm 0.82) \times 10^{-3}$	–	1.78 ± 0.19^a	1.80 ± 0.19^a
Grain amaranth	0.037 ± 0.008^a	–	6.99 ± 0.50^a	7.03 ± 0.52^a	1649.05 ± 260.38^a	1300.00 ± 100.00^a	$(1.21 \pm 0.32) \times 10^{-4}$	–	$(2.83 \pm 0.83) \times 10^{-3}$	–	1.81 ± 0.24^a	2.24 ± 0.32^a

The parameters are initial slope of the WUE_{inst}-I curve (α_2), coefficients β_2 and γ_2 and K_{inst}, the maximum instantaneous water-use efficiency ($WUE_{inst-max}$), and the corresponding saturation irradiance ($I_{inst-sat}$). All values are the means ± SE ($n = 4$). Different letters denote statistically significant differences ($P \leq 0.05$) between soybean and grain amaranth within each column of fitted (Eq. 10) or measured (Obs.) values. There is no statistically significant difference between fitted (Eq. 10) and measured (Obs.) values for each parameter. See ***Table 1*** *for definitions of abbreviations.*

contributing to the success of C_4 species in high irradiance environments (Pearcy and Ehleringer, 1984; Knapp, 1993).

Model Significance

By providing (1) analytical models characterizing the single-peaked light responses of WUE_i and WUE_{inst} and (2) key quantitative traits defining WUE_i–I and WUE_{inst}–I response differences between C_3 and C_4 species, this study provides a practical and robust modeling approach—in a form potentially applicable to WUE–I models at whole-plant and/or ecosystem scale. In particular, the key quantitative traits—the initial increase rates of WUE_i (α_1) and WUE_{inst} (α_2) besides that of A_n (α) and g_s (α_0), the maximum WUE_i (WUE_{i-max}) and WUE_{inst} ($WUE_{inst-max}$) besides that of A_n (A_{nmax}) and g_s (g_{s-max}), and the corresponding saturation irradiances—will directly help physiologists and modelers investigate the interrelationships among photosynthesis, stomatal behavior, and WUE under changing irradiance conditions.

Meanwhile, the above quantitative traits allow for easier and more extensive evaluation of light-intensity consequences on carbon and water relations among different species and/or PFTs. Such quantitative information, gathered on a wider range of species and/or PFTs, could allow (1) a deeper understanding of interspecific variation in light response strategies (Knapp, 1993; Hetherington and Woodward, 2003; McAusland et al., 2016), and (2) a realistic representation of adaptive WUE–I response differences among PFTs into ecosystem modeling.

The explicit models developed in this study can be viewed as an initial step toward filling the gap between investigating the trends of interspecific variation in short-term leaf-scale WUE–I responses and translating the variation into improved process representation in models of plant and ecosystem scales. The findings in this study remain to be validated (1) with species of different growth form and PFT membership (e.g., slower-growing woody species), which could hold different light response strategies (Knapp and Smith, 1989), (2) with daily and seasonal integrals and/or whole-plant estimates of WUE that sometimes could show a low correlation with short-term leaf-scale WUE observations (Medrano et al., 2015), and (3) when leaf gas exchange is subjected to compound effects of other climatic conditions in current and future climate change scenarios.

CONCLUSION

The newly developed models (Eqs. 7 and 10, respectively) allow robust reproduction of the differential single-peaked WUE_i–I and WUE_{inst}–I trends between C_3 and C_4 species and easy parameterization of key traits defining the trends (α_1, I_{i-sat}, K_i and WUE_{i-max}, α_2, $I_{inst-sat}$, K_{inst}, and $WUE_{inst-max}$). The models can be employed for fast and accurate assessment of plant WUE_i and WUE_{inst} responses—besides that of photosynthetic and stomatal responses using a consistent modeling framework—across all light-limited, light-saturated, and photoinhibitory light intensities. These findings are useful (1) for breeders screening for ideal genotypes target with maximized photosynthesis capacity and optimized WUE, (2) for plant physiologists quantifying

intra- and/or inter-specific variation in leaf-scale WUE–*I* responses, and (3) for modelers working on better representation of the coupling between carbon and water processes under dynamic irradiance conditions.

DATA AVAILABILITY STATEMENT

The datasets generated for this study are available on request to the corresponding author.

AUTHOR CONTRIBUTIONS

Z-PY and S-XZ drafted the work. All authors contributed substantially to the completion of this work and critically revised the work. Z-PY, H-JK, and Y-GL secured the funding.

FUNDING

This research was supported by the National Natural Science Foundation of China (Grant Nos. 31560069 and 31960054), the National Key Research and Development Program of China (Grant No. 2016 YFD 03001008), the Key Science and Technology Innovation Team Project of Wenzhou City (Grant No. C20150008), and the National Natural Science Foundation of China (Grant Nos. 31860045 and 31500583).

SUPPLEMENTARY MATERIAL

The Supplementary Material for this article can be found online at: https://www.frontiersin.org/articles/10.3389/fpls.2020.00374/full#supplementary-material

REFERENCES

Ahrar, M., Doneva, D., Tattini, M., Brunetti, C., Gori, A., Rodeghiero, M., et al. (2017). Phenotypic differences determine drought stress responses in ecotypes of *Arundo donax* adapted to different environments. *J. Exp. Bot.* 68, 2439–2451. doi: 10.1093/jxb/erx125

Aranda, I., Pardos, M., Puértolas, J., Jiménez, M. D., and Pardos, J. A. (2007). Water-use efficiency in cork oak (*Quercus suber*) is modified by the interaction of water and light availabilities. *Tree Physiol.* 27, 671–677. doi: 10.1093/treephys/27.5.671

Avola, G., Cavallaro, V., Patanè, C., and Riggi, E. (2008). Gas exchange and photosynthetic water use efficiency in response to light, CO2 concentration and temperature in *Vicia faba*. *J. Plant Physiol.* 165, 796–804. doi: 10.1016/j.jplph.2007.09.004

Baly, E. C. (1935). The kinetics of photosynthesis. *Philos. R. Soc. Lond. B* 117, 218–239. doi: 10.1098/rspa.1935.0083

Bota, J., Tomás, M., Flexas, J., Medrano, H., and Escalona, J. M. (2016). Differences among grapevine cultivars in their stomatal behavior and water use efficiency under progressive water stress. *Agrcult. Water Manage.* 164, 91–99. doi: 10.1016/j.agwat.2015.07.016

Buckley, T. N., and Mott, K. A. (2013). Modelling stomatal conductance in response to environmental factors. *Plant Cell Environ.* 36, 1691–1699. doi: 10.1111/pce.12140

Buckley, T. N., Mott, K. A., and Farquhar, G. D. (2003). A hydromechanical and biochemical model of stomatal conductance. *Plant Cell Environ.* 26, 1767–1785. doi: 10.1046/j.1365-3040.2003.01094.x

Chen, X., Liu, W. Y., Song, L., Li, S., Wu, C. S., and Lu, H. Z. (2016). Adaptation of epiphytic bryophytes in the understorey attributing to the correlations and trade-offs between functional traits. *J. Bryol.* 38, 110–117. doi: 10.1080/03736687.2015.1120370

De Kauwe, M. G., Zhou, S. X., Medlyn, B. E., Pitman, A. J., Wang, Y. P., Duursma, R. A., et al. (2015). Do land surface models need to include differential plant species responses to drought? Examining model predictions across a mesic-xeric gradient in Europe. *Biogeosciences* 12, 7503–7518. doi: 10.5194/bg-12-7503-2015

Dewar, R. O. (2002). The Ball–Berry–Leuning and Tardieu–Davies stomatal models: synthesis and extension within a spatially aggregated picture of guard cell function. *Plant Cell Environ.* 25, 1383–1398. doi: 10.1046/j.1365-3040.2002.00909.x

dos Santos, J. U. M., de Carvalho, G. J. F., and Fearnside, P. M. (2013). Measuring the impact of flooding on Amazonian trees: photosynthetic response models for ten species flooded by hydroelectric dams. *Trees* 27, 193–210. doi: 10.1016/j.agrformet.2012.09.005

Dudley, S. A. (1996). Differing selection on plant physiological traits in response to environmental water availability: a test of adaptive hypotheses. *Evolution* 50, 92–102. doi: 10.1111/j.1558-5646.1996.tb04475.x

Duursma, R. A., Payton, P., Bange, M. P., Broughton, K. J., Smith, R. A., Medlyn, B. E., et al. (2013). Near-optimal response of instantaneous transpiration efficiency to vapour pressure deficit, temperature and [CO2] in cotton (*Gossypium hirsutum* L.). *Agr. Forest Meteorol.* 168, 168–176. doi: 10.1016/j.agrformet.2012.09.005

Eamus, D., Huete, A., and Yu, Q. (2016). *Vegetation Dynamics: A Synthesis of Plant Ecophysiology, Remote Sensing and MODELLINg*. Cambridge: Cambridge University Press, 331–333.

Egea, G., Verhoef, A., and Vidale, P. L. (2011). Towards an improved and more flexible representation of water stress in coupled photosynthesis–stomatal conductance models. *Agr. Forest Meteorol.* 151, 1370–1384. doi: 10.1016/j.agrformet.2011.05.019

Fischer, R. A., and Turner, N. C. (1978). Plant productivity in the arid and semiarid zones. *Annu. Rev. Plant Biol.* 29, 277–317. doi: 10.1146/annurev.pp.29.060178.001425

Flexas, J., Niinemets, U., Gallé, A., Barbour, M. M., Centritto, M., Diaz-Espejo, A., et al. (2013). Diffusional conductances to CO2 as a target for increasing photosynthesis and photosynthetic water-use efficiency. *Photosyn. Res.* 117, 45–59. doi: 10.1007/s11120-013-9844-z

Gilbert, M. E., Zwieniecki, M. A., and Holbrook, N. M. (2011). Independent variation in photosynthetic capacity as stomatal conductance leads to differences in intrinsic water use efficiency in 11 soybean genotypes before and during mild drought. *J. Exp. Bot.* 62, 2875–2887. doi: 10.1093/jxb/erq461

Gomes, F. P., Oliva, M. A., Mielke, M. S., Almeida, A. A. F., and Leite, H. G. (2006). Photosynthetic irradiance-response in leaves of dwarf coconut palm (*Cocos nucifera* L. 'nana'. Araceae): comparison of three models. *Sci. Hortic.* 109, 101–105. doi: 10.1016/j.scienta.2006.02.030

Hetherington, A. M., and Woodward, F. I. (2003). The role of stomata in sensing and driving environmental change. *Nature* 424, 901–908. doi: 10.1038/nature01843

Knapp, A. K. (1993). Gas exchange dynamics in C3 and C4 grasses: consequence of differences in stomatal conductance. *Ecology* 74, 113–123. doi: 10.2307/1939506

Knapp, A. K., and Smith, W. K. (1987). Stomatal and photosynthetic responses during sun/shade transitions in subalpine plants: influence on water use efficiency. *Oecologia* 74, 62–67. doi: 10.1007/BF00377346

Knapp, A. K., and Smith, W. K. (1989). Influence of growth form and water relations on stomatal and photosynthetic responses to variable sunlight in subalpine plants. *Ecology* 70, 1069–1082. doi: 10.2307/1941376

Knapp, A. K., and Smith, W. K. (1990). Stomatal and photosynthetic responses to variable sunlight. *Physiol. Plant* 78, 160–165. doi: 10.1111/j.1399-3054.1990.tb08731.x

Köhler, I. H., Macdonald, A. J., and Schnyder, H. (2016). Last-century increases in intrinsic water-use efficiency of grassland communities have occurred over a wide range of vegetation composition, nutrient inputs, and soil PH. *Plant Physiol.* 170, 881–890. doi: 10.1104/pp.15.01472

Linares, J. C., and Camarero, J. J. (2012). From pattern to process: linking intrinsic water-use efficiency to drought-induced forest decline. *Glob. Change Biol.* 18, 1000–1015. doi: 10.1111/j.1365-2486.2011.02566.x

Ludlow, M. M., and Wilson, G. L. (1972). Photosynthesis of tropical pasture plants. IV. Basis and consequences of differences between grasses and legumes. *Aust. J. Biol. Sci.* 25, 1133–1145. doi: 10.1071/BI9721133

McAusland, L., Vialet-Chabrand, S., Davey, P., Baker, N. R., Brendel, O., and Lawson, T. (2016). Effects of kinetics of light-induced stomatal responses on photosynthesis and water-use efficiency. *New Phytol.* 211, 1209–1220. doi: 10.1111/nph.14000

Medlyn, B. E., De Kauwe, M., Lin, Y. S., Knauer, J., Duursma, R. A., Williams, C. A., et al. (2017). How do leaf and ecosystem measures of water-use efficiency compare? *New Phytol.* 216, 758–770. doi: 10.1111/nph.14626

Medrano, H., Tomás, M., Martorell, S., Flexas, J., Hernández, E., Rosselló, J., et al. (2015). From leaf to whole-plant water use efficiency (WUE) in complex canopies: limitations of leaf WUE as a selection target. *Crop J.* 3, 220–228. doi: 10.1016/j.cj.2015.04.002

Mott, K. A. (1988). Do stomata respond to CO2 concentrations other than intercellular? *Plant Physiol.* 86, 200–203. doi: 10.1104/pp.86.1.200

Pearcy, R. W., and Ehleringer, J. (1984). Comparative ecophysiology of C3 and C4 plants. *Plant Cell Environ.* 7, 1–13. doi: 10.1111/j.1365-3040.1984.tb01194.x

Sinclair, T. R., Tanner, C. B., and Bennett, J. M. (1984). Water-use efficiency in crop production. *Bioscience* 34, 36–40. doi: 10.2307/1309424

Smith, W. K., Knapp, A. K., and Reiners, W. A. (1989). Penumbral effects on sunlight penetration in plant communities. *Ecology* 70, 1603–1609. doi: 10.2307/1938093

Song, L., Zhang, Y. J., Chen, X., Li, S., Lu, H. Z., Wu, C. S., et al. (2015). Water relations and gas exchange of fan bryophytes and their adaptations to microhabitats in an Asian subtropical montane cloud forest. *J. Plant Res.* 128, 573–584. doi: 10.1007/s10265-015-0721-z

Thornley, J. H. M. (1976). *Mathematical Models in Plant Physiology*. London: Academic Press, 86–110.

von Caemmerer, S., and Farquhar, G. D. (1981). Some relationships between the biochemistry of photosynthesis and the gas exchange of leaves. *Planta* 153, 376–387. doi: 10.1007/BF00384257

Wargent, J. J., Elfadly, E. M., Moore, J. P., and Paul, N. D. (2011). Increased exposure to UV-B radiation during early development leads to enhanced photoprotection and improved long-term performance in *Lactuca sativa*. *Plant Cell Environ.* 34, 1401–1413. doi: 10.1111/j.1365-3040.2011.02342.x

Webster, R. J., Driever, S. M., Kromdijk, J., McGrath, J., Leakey, A. D. B., Siebke, K., et al. (2016). High C3 photosynthetic capacity and high intrinsic water use efficiency underlies the high productivity of the bioenergy grass *Arundo donax*. *Sci. Rep.* 6:20694. doi: 10.1038/srep20694

Xu, Z. F., Hu, T. X., and Zhang, Y. B. (2012a). Effects of experimental warming on phenology, growth and gas exchange of treeline birch (*Betula utilis*) saplings. Eastern Tibetan Plateau, China. *Eur. J. Forest Res.* 131, 811–819. doi: 10.1007/s10342-011-0554-9

Xu, Z. F., Yin, H. J., Xiong, P., Wan, C., and Liu, Q. (2012b). Short-term responses of Picea asperata seedlings of different ages grown in two contrasting forest ecosystems to experimental warming. *Environ. Exp. Bot.* 77, 1–11. doi: 10.1016/j.envexpbot.2011.10.011

Ye, Z. P. (2007). A new model for relationship between irradiance and the rate of photosynthesis in *Oryza sativa*. *Photosynthetica* 45, 637–640. doi: 10.1007/s11099-007-0110-5

Ye, Z. P., Suggett, J. D., Robakowski, P., and Kang, H. J. (2013). A mechanistic model for the photosynthesis-light response based on the photosynthetic electron transport of PS II in C3 and C4 species. *New Phytol.* 152, 1251–1262. doi: 10.1111/nph.12242

Ye, Z. P., and Yu, Q. (2008). A coupled model of stomatal conductance and photosynthesis for winter wheat. *Photosynthetica* 46, 637–640. doi: 10.1007/s11099-008-0110-0

Zhou, S., Medlyn, B., Sabaté, S., Sperlich, D., and Prentice, I. C. (2014). Short-term water stress impacts on stomatal, mesophyll and biochemical limitations to photosynthesis differ consistently among tree species from contrasting climates. *Tree Physiol.* 34, 1035–1046. doi: 10.1093/treephys/tpu072

Zhou, S.-X., Medlyn, B. E., and Prentice, I. C. (2016). Long-term water stress leads to acclimation of drought sensitivity of photosynthetic capacity in xeric but not riparian Eucalyptus species. *Ann. Bot.* 117, 133–144. doi: 10.1093/aob/mcv161

Zhou, S.-X., Prentice, I. C., and Medly, B. E. (2019). Bridging drought experiment and modelling: representing the differential sensitivities of leaf gas exchange to drought. *Front. Plant Sci.* 9:1965. doi: 10.3389/fpls.2018.01965

Conflict of Interest: The authors declare that the research was conducted in the absence of any commercial or financial relationships that could be construed as a potential conflict of interest.